R. & M. No. 3155
(20,036)
A.R.C. Technical Report

MINISTRY OF AVIATION

AERONAUTICAL RESEARCH COUNCIL
REPORTS AND MEMORANDA

The Effects of Distributed Suction on the Development of Turbulent Boundary Layers

By R. A. DUTTON
ENGINEERING LABORATORY, CAMBRIDGE

LONDON: HER MAJESTY'S STATIONERY OFFICE
1960
PRICE 11*s.* 0*d.* NET

The Effects of Distributed Suction on the Development of Turbulent Boundary Layers

By R. A. Dutton

Engineering Laboratory, Cambridge

Reports and Memoranda No. 3155

March, 1958

Summary. Experiments have been performed on the turbulent boundary layer with uniform suction and with zero pressure gradient. The test surface consisted of a uniformly perforated sheet which replaced the floor of a wind tunnel, the tunnel boundary layer being removed through a slot a short distance ahead of the test section. For several different suction velocities, and for different entry conditions, boundary-layer measurements were made on the perforated surface and on a porous surface formed by covering the perforated sheet with calendered nylon fabric.

For certain conditions it was found that both the thickness and the velocity profile of the turbulent boundary layer remained constant over virtually the full length of the suction surface, thus establishing the existence of a turbulent asymptotic layer. At sufficiently high rates of suction it was found that an initially turbulent layer reverted to the laminar asymptotic form.

1. *Introductory.* 1.1. *Introduction.* Almost all the fundamental work on boundary-layer control by distributed suction has been confined to laminar boundary layers. There has been a considerable amount of *ad hoc* testing in which suction has been applied to the turbulent boundary layer to prevent separation, but very few experiments have been performed to show the general behaviour of the turbulent boundary layer with suction, or to provide the basis for methods of calculation. Control of turbulent boundary layers is needed primarily to prevent separation and provided it is economical it may be used to considerable advantage to increase the lift on aerofoils, particularly by maintaining unseparated flow over flaps (*see*, for example, Ref. 1), and to improve the flow in air intakes and diffusers.

As implied above a few basic experiments have been carried out and there have been two attempts to provide a theory for the rather special case where the suction is uniformly distributed and the turbulent boundary layer develops over a flat plate with zero pressure gradient. The first was by Schlichting[2] and this was followed some years later by a more detailed theory proposed by Kay[3]. Both of these have been guided by a knowledge of the corresponding laminar boundary-layer behaviour and therefore before describing them it will be useful to review very briefly the principal result of previous studies of the laminar boundary-layer problem.

It was found by Griffith and Meredith[4] that a particularly simple, exact solution existed for a flat plate with uniformly distributed suction. It was assumed that sufficiently far downstream the rate of growth of the laminar boundary layer due to skin friction could be balanced exactly by the rate of decrease due to suction, and that the distribution of velocity in the boundary layer would

assume a form independent of the distance from the leading edge; this simplified the boundary-layer equations to such an extent that an exact relation could be obtained for the asymptotic profile. Experiments made by Kay on a flat porous plate of sintered bronze, with zero pressure gradient, established this result and also showed that the laminar boundary-layer velocity profile with suction rapidly approached the asymptotic form predicted by the theory.

After this result had been obtained for the laminar boundary-layer, it was natural to suppose that a similar balance between the rate of boundary-layer growth due to skin friction and the rate of decrease due to suction could be achieved when the boundary layer was turbulent, and the theories already referred to were developed by making this assumption.

Schlichting, using the momentum equation and assuming that the skin friction on the porous surface could be obtained in terms of R_θ (Reynolds number based on momentum thickness) from the existing solid flat-plate empirical law, obtained a solution for the asymptotic value of R_θ in terms of the suction-velocity ratio.

Kay also assumed the existence of an asymptotic solution and suggested that the profile could be divided into two parts: an inner part which could be represented by the laminar asymptotic profile for the same rate of suction, and an outer part which could be described by an equation derived from the simplified equations of motion and a mixing-length theory. However, the experiments made to test this theory were not very conclusive, because of the small number of experimental results and the limited extent of the porous plate. Consequently the existence of a turbulent asymptotic profile was by no means established when the present investigation was undertaken.

The experiments to be described in this paper (a brief description of these experiments is also given in Ref. 5) were carried out to provide a general picture of the effects of uniformly distributed suction on the development of the two-dimensional turbulent boundary layer over a flat porous surface. It was intended to prove or disprove the existence of the asymptotic turbulent boundary layer, and to investigate as many as possible of the parameters likely to affect the growth of the turbulent boundary layer with suction. Although, as has already been mentioned, control of the turbulent boundary layer is useful chiefly in preventing separation due to adverse pressure gradients, it was considered advisable to investigate first the boundary-layer development under the simplest possible conditions, *i.e.*, with zero pressure gradient.

To provide a basis for comparison, experiments were first made to investigate the boundary-layer development over the plate without suction.

1.2. *Dimensional Analysis of the Problem.* If uniform suction is applied to a continuously porous flat plate following a short solid entry section, then at any point along the plate the boundary-layer momentum thickness θ may be expected to depend upon the following:

(i) Relevant properties of the fluid

(ii) Distance along the plate

(iii) Thickness of the boundary layer at the commencement of suction

(iv) Shape of the velocity profile at the commencement of suction

(v) Free-stream velocity

(vi) Suction velocity,

or expressed symbolically

$$\theta = f(\rho,\mu,x,\theta_0,H_0,U_1,V_s)\,. \tag{1}$$

This function of seven parameters may be expressed as

$$R_\theta = F\left(R_x, \frac{V_s}{U_1}, R_{\theta\,0}, H_0\right) . \tag{2}$$

If the pressure gradient is zero over the solid entry length, then H_0 can be expressed as a function of $R_{\theta\,0}$, and equation (2) reduces to

$$R_\theta = F\left(R_x, \frac{V_s}{U_1}, R_{\theta\,0}\right) . \tag{3}$$

However, if the surface is perforated, instead of being continuously porous, further relevant variables must be considered. It is to be expected that the diameter of the perforations, their spacing and the general pattern in which they are arranged, will need to be introduced. If the spacing and general pattern can be specified by a single non-dimensional parameter P, then equation (3) becomes

$$R_\theta = F\left(R_x, \frac{V_s}{U_1}, R_{\theta\,0}, R_d, P\right) , \tag{4}$$

where R_d is the Reynolds number based on the hole diameter d, and stream velocity.

In the present investigation two types of surface were used, first a perforated surface in which the holes were approximately uniform in size and spaced one diameter apart, and second this same surface covered with smooth calendered nylon. With the second surface the effective hole diameter was considerably decreased, and in addition the hole pattern was changed because the holes in the nylon were superimposed on those in the perforated surface below.

2. *Description of Apparatus and Procedure.* 2.1. *General Arrangement.* The experiments to be described were carried out in the working-section of a wind tunnel. The solid floor of the working-section was replaced by a 6 ft × 1 ft 8 in. finely perforated brass sheet, rigidly supported, through which suction could be applied. The arrangement is shown diagrammatically in Fig. 1. The perforated surface was preceded by a 4·15 in. solid entry length which formed the upper lip of a bleed through which the tunnel boundary layer was removed.

To ensure uniformity of the suction flow, which would otherwise have been influenced by small pressure variations along the surface, the perforated brass sheet was backed by a sheet of blotting paper supported by a second perforated sheet, the holes in this being 0·080 in. diameter as compared with 0·020 in. in the upper perforated sheet. The two perforated sheets with the blotting paper sandwiched between them were stretched on the metal supporting frame shown in Fig. 2. The region below the lower perforated sheet was divided by longitudinal partitions into three compartments which opened into a single small reservoir connected to the pump inlet. Each of the three openings was fitted with a shutter which provided a control on the suction flow from that compartment. The pump used for the suction was a Rolls-Royce Merlin supercharger, run at half speed and delivering approximately 1,000 cu ft/min, with a pressure rise across it of about 6 in. mercury. For the existing arrangement this provided suction velocities through the perforated surface up to 0·75 ft/sec. The suction flow was controlled by a butterfly valve on the pump inlet. It was not practicable to investigate the effects of a change in the nature of the surface by replacing the outer perforated sheet with one with different diameter holes or different hole spacing. Instead, a comparison was made between the results obtained on the existing perforated sheet and those obtained on an almost continuously porous surface, by covering the perforated sheet with smooth calendered nylon. The upstream edge of this nylon was fixed just ahead of the first row of perforations

and the remainder was held down in each test by the suction. The difference in the geometry of the two surfaces can be seen from Figs. 3 and 4 which show photographs of the perforated sheet and the calendered nylon magnified 10 and 75 times respectively.

The pressure gradient was adjusted approximately to zero by changing the inclination of the roof of the tunnel working-section. The final pressure distribution obtained is shown in Fig. 5, where it will be seen that a favourable gradient exists over the first few inches and after a small adverse pressure gradient the variation of the static pressure over the remainder of the plate is approximately $\frac{1}{2}$ per cent q_0 about a mean.

Transition was promoted in the boundary layer by fixing a wire 0·020 in. in diameter, on the surface 0·65 in. back from the leading edge.

2.2. *Measurement of Mean Velocities and Pressures.* The absolute local suction velocities through the surface were measured using a deflecting-vane anemometer, which was calibrated by measuring a displaced volume of water. With this, velocities in the range 0·10 to 0·80 ft/sec could be measured with an estimated accuracy of about ± 5 per cent.

Almost all the boundary-layer profiles were measured using a pitot comb in conjunction with a multi-tube tilting manometer. The pitot comb is shown in Fig. 6. The twelve pitot-tubes in the comb were made of hypodermic tubing, the ends being flattened and ground until their external dimensions were, width 0·060 in., and depth 0·010 in. The results obtained with the comb and the multi-tube manometer agreed very well with traverses made by a single fine flattened pitot-tube (width 0·060 in., depth 0·006 in.), but the latter was used in preference to the comb for measurements in the thin boundary layers obtained with large suction velocities. The free-stream dynamic pressure at each station was obtained from pitot and static tubes attached to the comb (*see* Fig. 6) in such a way that they were well outside the boundary layer in all experiments.

The static-pressure distribution was obtained by traversing a static tube, 0·040 in. in diameter, along the centre-line of the plate at a height of 0·050 in. above the surface.

All experiments were made at a constant Reynolds number per foot, the tunnel speed being varied as required to take account of the changes in temperature and pressure in the working-section. This was done in an attempt to ensure that the effects of the transition wire and the appropriate non-dimensional parameters appearing in equation (4) would remain constant throughout the investigation.

No corrections were applied for the displacement of the effective centre of the pitot-tube, as this was believed to have a negligible effect on the values of momentum thickness calculated from the velocity profiles.

3. *Description of Experiments.* 3.1. *Preliminary Experiments Without Suction.* These experiments were carried out to check that in the absence of suction the development of the turbulent boundary layer was closely two-dimensional and that its rate of growth compared closely with established laws.

In the initial experiments the rate of growth as checked on the exposed perforated surface was some 20 per cent greater than would follow from the accepted skin-friction laws. This discrepancy was approximately halved by covering the perforated surface with tracing linen which eliminated the possibility of outflow occuring through the surface. The remaining discrepancy was virtually eliminated by removing the transition wire which was found to be redundant, a naturally occurring

laminar separation at the nose of the plate ensuring that transition took place within $\frac{1}{4}$ in. of the leading edge.

Small discrepancies were observed between profiles measured five in. on either side of the centre-line 41 in. back along the plate (*see* Fig. 7). By applying a high rate of suction at the edges of the tracing linen it was established that these discrepancies (which were only of the order of 2 per cent in momentum thickness), were not due to secondary flows from the tunnel walls and no serious attempt was made to reduce their magnitude.

From these experiments it was concluded that the experimental arrangement was satisfactory for the proposed tests.

3.2. *Experiments with Fixed Entry Conditions and Variable Suction Ratio.* 3.2.1. *Description of experiments.* Preliminary experiments were made to obtain a uniform distribution of suction through the perforated surface. By adjusting the shutters between the three compartments and the suction box, a distribution of suction velocity was obtained which varied only by approximately $\pm$ 5 per cent about a mean. Owing to the possibility of the blotting paper backing the perforated sheet becoming blocked with dust, and leaks developing in the system, the calibration was repeated fairly often.

For the experiments made with the perforated surface completely covered with calendered nylon, a fresh calibration was made. Again this had to be frequently checked because after a relatively short running period the resistance of the nylon changed appreciably.

Following these preliminary experiments, boundary-layer velocity profiles were measured at close intervals along the centre-line of the plate, for suction ratios v_s/U_1 varying from 0·00443 to the maximum value of 0·0125. A similar series of measurements with approximately the same suction ratios were then made on the nylon-covered surface.

Later, after these results had been obtained and the values of R_θ computed, experiments were made on each surface for the critical suction ratios found by cross-plotting the above results in the form R_θ vs. V_s/U_1, for constant values of R_x.

3.2.2. *Results.* The results obtained with uniformly distributed suction through the perforated surface are shown in Fig. 8, where they are plotted in the form suggested by equation (4), i.e., R_θ vs. R_x for constant values of R_d, $R_{\theta\,0}$ and P, and where they are also compared with the results obtained with zero suction. At once it is apparent that the general behaviour of the turbulent boundary layer with suction is somewhat different from that which might have been expected from a knowledge of laminar boundary layers. For values of V_s/U_1 less or greater than a certain critical value there is no tendency, at least over the length of the present perforated plate, for the boundary layer to reach a state in which the value of R_θ and the profile shape remain constant. For a laminar boundary layer with the same suction ratios a constant state would very quickly be reached. This may well be due to the fact that C_f varies much less rapidly with R_θ for the turbulent than for the laminar layer.

Fig. 9 shows the change in the velocity profile shape with suction ratio at a fixed value of R_x ($9{\cdot}75 \times 10^5$). As the ratio V_s/U_1 increases the profile shape divides into two distinct parts, an inner part which resembles the laminar asymptotic profile and an outer part which takes the form of a long thin 'tail' which only slowly diminishes. However, the fact that it does decay, and that, for ratios of V_s/U_1 greater than a critical value, R_θ continually diminishes, suggested that the boundary

layer might eventually reach the laminar asymptotic state. This was indeed found to be the case near the rear of the plate with the maximum suction available. Fig. 10 compares the velocity profiles measured in this region with the calculated laminar asymptotic profile. The long turbulent tail which was seen in Fig. 9 to diminish with increasing suction has been eliminated and the profiles which remain agree closely with the calculated one.

When the above results were cross-plotted in the form R_θ vs. V_s/U_1 for constant values of R_x, it was found that the curves all intersected at a common point, thus indicating that conditions did exist in which R_θ would remain constant over the perforated surface, and giving the necessary value of V_s/U_1 to produce these conditions. It proved to be very difficult to control the suction flow with sufficient accuracy to maintain the constant boundary-layer state, but eventually this was achieved and the results included in Fig. 8 were obtained. Under these conditions the profile quickly assumed a constant shape and thus a true turbulent asymptotic suction profile was obtained.

The results of the experiments on the nylon-covered surface are shown in Fig. 11, and are compared with the results obtained without suction on the tracing linen.

The general effect of suction is the same as on the perforated surface but now it is seen that the suction quantities required to produce equal reductions in R_θ (at a particular R_x) are much less than before, and this is particularly so for the smaller rates of suction. Again it is noticed that the boundary layer does not tend towards a constant form for each particular set of conditions. Also, although the laminar asymptotic boundary layer is once more achieved, the suction ratio necessary is not very much less than that required on the perforated surface. The critical suction conditions under which R_θ and profile shape remained constant all along the surface, were found in the same way as on the perforated surface, and are included in Fig. 11.

An interesting feature of these results is seen from Fig. 12, which compares the turbulent asymptotic profile on nylon with that on the perforated surface. In spite of the quite different suction ratios required to produce the constant condition on the two surfaces, the values of R_θ are the same and the resultant asymptotic profiles are identical except in the immediate vicinity of the wall, where they are necessarily different because of the different values of skin friction.

3.3. *Experiments with the Critical Suction Velocity Ratio and Variable Entry Conditions.*
3.3.1. *Description of experiments.* In Section 1.2 it was shown that, in the general case, the Reynolds number based on momentum thickness at any point is given by

$$R_\theta = f\left(R_x, \frac{V_s}{U_1}, R_d, R_{\theta 0}, P\right). \tag{4}$$

In the experiments just described the last three parameters were kept constant for each surface tested and V_s/U_1 varied. In the following experiments $R_{\theta 0}$ was varied by altering the entry length and V_s/U_1 was kept constant at the value required to maintain the asymptotic turbulent boundary layer with the original entry conditions. This value was, as remarked earlier, different for the two types of surface tested.

Initially, the existing solid entry length of 4·15 in. was increased by covering the required length of perforated or nylon-covered surface with thin cellophane, but it was found later that for some of the entry lengths chosen this resulted in a very high suction velocity at the downstream edge of the cellophane. This was due to the blotting-paper backing being sucked away in this region from the under surface of the perforated sheet. Some doubt was therefore thrown on the results obtained

in this way and a different method of increasing the entry length was later adopted. Aluminium sheets of various lengths were attached to the plate leading edge and allowed to extend forward towards the tunnel contraction.

Experiments were made on both surfaces with the suction-velocity ratio for each surface adjusted to the value found earlier to give asymptotic conditions with the solid entry length, a series of velocity profiles being measured along the plate centre-line for each particular set of entry conditions.

3.3.2. *Results.* The results obtained on the perforated surface using both methods of increasing the solid entry length are shown in Figs. 13a and 13b. As shown by Fig. 13a the increased suction at the downstream edge of the cellophane did not have any appreciable influence on the general behaviour of the boundary layer. The measurements made with double the original solid entry length show that a constant value of R_θ is again rapidly approached and this constant R_θ is approximately the same as the original asymptotic R_θ. With the entry length four times as long a constant state is not achieved although R_θ decreases continually over the whole length of plate.

The boundary-layer velocity profiles measured along the surface, when the entry length was increased with the cellophane sheets, are compared with the original asymptotic profile in Figs. 14a, 14b and 14c. When the entry length was doubled, the profiles beyond a certain distance from the leading edge agreed closely with the asymptotic profile, as would be expected, but this was not so when the entry length was increased still further. The velocity profiles then continually change shape and do not approach the original asymptotic one.

On the nylon-covered surface the behaviour of the boundary layer is very different. The results of these experiments are shown in Figs. 15a and 15b and there it is seen that with the critical suction ratio and for each particular entry condition the value of R_θ remains substantially constant over the whole plate, and is closely related to the particular value at the beginning of suction. Although R_θ is constant along the plate for each set of conditions the velocity profile shape is continually changing as is shown in Figs. 16a, 16b and 16c, where the velocity profiles are plotted for the conditions corresponding to those for Fig. 15a. Towards the rear of the plate the change in profile shape is less marked but there is no tendency for the final profile, even for the doubled entry length, to approach the original asymptotic profile.

3.4. *General Discussion.* It is evident from the results of the above experiments that the turbulent boundary layer on a flat plate with suction presents a much more complex problem than the corresponding laminar boundary layer. There, the boundary layer is known to approach a constant form very quickly after the commencement of suction and the asymptotic velocity profile is determined simply by the suction velocity V_s. No such general asymptotic solution appears to exist for the turbulent boundary layer. The general boundary-layer behaviour depends appreciably on the surface characteristics and the state of the layer at the commencement of suction.

However, it has been shown that under certain special conditions an asymptotic solution does exist for the turbulent boundary layer. The critical suction ratio required to maintain the constant state in the boundary layer is to a large extent dependent on the nature of the porous surface. Also, whether the boundary layer will reach a constant form or not, even with the critical suction ratio, is found to depend on the initial entry conditions which again appear to influence the flow more on one type of surface than on the other. The final state reached by the boundary layer, with the critical suction ratio and various entry conditions, is discussed later in this Section.

Another important result is that the turbulent boundary layer can be reduced to the laminar asymptotic form, although this state is approached only slowly and requires a large amount of suction. It should be noted that, while for the smaller suction ratios a certain suction quantity through the nylon-covered surface will thin the boundary layer much more effectively than the same quantity through the perforated surface, the laminar asymptotic state is reached by applying almost the same high suction ratio to each surface.

The different values of the suction velocity required to achieve an asymptotic turbulent layer on the two types of surface can perhaps be explained in the following way: The flow about and into the holes in the perforated surface is such that the surface has an effective roughness, and due to this the skin friction is high; consequently the suction necessary to maintain a particular boundary-layer thickness is greater than on the smooth nylon-covered surface.

This also goes some distance towards explaining the different results observed with the two surfaces for various lengths of solid entry. Comparing the results for the perforated and porous surfaces, with double the original entry length (Figs. 13 and 15), it will be seen that for the perforated surface the boundary layer approaches rapidly the asymptotic form achieved with the original entry length, while for the porous surface this was not the case. We might assume that for the perforated surface the higher rate of suction ($V_s/U_1 = 0{\cdot}0073$ as against $0{\cdot}0044$) was responsible for the relatively rapid initial thinning, due to the roughness effect being relatively unimportant until the boundary layer was reduced in thickness to something like the asymptotic value. A similar effect (*i.e.*, a noticeably increased rate of thinning) will also be observed for the perforated surface where the entry length has been increased four times, though here, over the full length of the plate, there is still no close approach to the original asymptotic condition.

With the porous surface it will be observed that with any increased length of solid entry there is no evidence of any close approach to the original asymptotic condition; not only does the momentum thickness remain virtually constant at only slightly less than the initial value, but the velocity profiles appear to tend in shape away from, rather than towards, that of the original asymptotic profile. Indeed it appears that for a given suction velocity ratio and a given surface, several asymptotic forms of the turbulent boundary layer may be possible depending on the length of solid entry. If this is the case, then it is a somewhat remarkable result, since it implies that under identical equilibrium conditions several alternative forms of the turbulent boundary layer may be obtained, all with the same skin friction.

In an attempt to describe quantitatively the changes in profile shape taking place along the plate, which are immediately obvious from Figs. 14 and 16, values of H were determined for the set of profiles shown in Fig. 14c. Somewhat surprisingly it was found that H varied very little and such variation as evidently must have occurred was almost obscured by scatter of the experimental points. It was therefore concluded that the parameter H is not well suited to describing the shape of profiles where, as in the present case, the values of u/U_1 lie between $0{\cdot}9$ and $1{\cdot}0$ over a large part of the boundary-layer thickness.

It is interesting to note that the measured asymptotic profiles obtained on the two types of surface were identical except in a region very close to the surface, while the suction velocity ratios for the two profiles were very different. This is another somewhat surprising result, suggesting as it does that in the asymptotic conditions the major part of the profile shape is independent of the skin friction.

4. *Detailed Examination of the Asymptotic Turbulent Boundary Layer.* 4.1. *Comparison between Experimental Results and the Work of Schlichting and Kay.* It is obvious that the results obtained on the perforated surface cannot agree closely with existing theories because these do not take into account the effects of variations in the nature of the surface. It might be hoped that better agreement would be obtained in the case of the nylon-covered surface which approximated much more closely to a continuously porous surface, but the dependence of the asymptotic results on the boundary-layer Reynolds number at the commencement of suction (another item unaccounted for by the existing theories), suggested that very good agreement could not be expected. Nevertheless, it was considered worthwhile to compare the results obtained with the nylon surface with the results from the semi-empirical theories, to see whether either of these could be regarded as being approximately correct.

4.1.1. *Comparison with Schlichting's results.* The chief assumption made in Schlichting's analysis was that the distribution of skin friction along the surface through which suction was applied could be obtained in terms of R_θ, from the empirical relationship for a turbulent boundary layer without suction. The results of the experiments with the original solid entry length (Figs. 15a and 15b), show clearly that this assumption is incorrect. There the value of R_θ at the beginning of suction is exactly the same as the final asymptotic value while the skin friction at the beginning of suction (found from dR_θ/dR_x) is approximately one third of that for the final asymptotic state.

Because of this the agreement with Schlichting's formula for the asymptotic value of $R_\theta(R_{\theta\,\infty})$ is very poor, the calculated value being approximately 10 compared with the measured value of 680. The reason for this large discrepancy is that any errors appearing in the formula for τ_0 are greatly increased when this is raised to the fourth power to give $R_{\theta\,\infty}$.

4.1.2. *Comparison with Kay's theory.* It has already been mentioned that by using the equations of motion for turbulent boundary-layer flow, and Taylor's vorticity transfer theory, Kay was able to show that the turbulent asymptotic profile could be divided into two parts. The inner part is represented by the laminar asymptotic boundary layer and the outer part has the form

$$\frac{u}{U_1} = 1 + \frac{1}{k^2}\frac{V_s}{U_1}\log_e\frac{y}{\delta},$$

where k is a constant to be derived from experiment and found by Kay to be approximately 0·23. Again, this expression takes no account of the effects caused by the nature of the surface and entry conditions.

The outer part of the present asymptotic profile will lie on a straight line when plotted in the above form, but the value of k will be different because of the different conditions. For the nylon-covered surface it is found to be 0·31, which differs considerably from Kay's result but is nearer the value of 0·36 which is normally assumed for the Kármán similarity theory for fully developed pipe flow.

Kay assumed that the distribution of Reynolds stress through the asymptotic layer would be the same as in the ordinary turbulent boundary layer and could be given by an equation based on Taylor's vorticity-transfer theory. For the special asymptotic conditions the Reynolds stress distribution can be calculated from the velocity profile (*see* Appendix) and it is of interest now to compare this with the Reynolds stress distribution measured by Klebanoff[7] in a turbulent boundary

layer on a solid flat plate. Both the Reynolds stresses and the viscous stresses are shown in Fig. 17. The distribution of the stresses in the two types of boundary layer are quite different and this is particularly applicable to the Reynolds stress distribution. This therefore provides another objection to Kay's theory.

From the above it will be seen that there are several difficulties to be overcome before an equation can be derived which will accurately describe the asymptotic turbulent boundary layer.

4.2. *Comparison with the Logarithmic 'Inner' Law for Turbulent Boundary-Layer Profiles.* For the asymptotic turbulent boundary layer with suction the skin friction along the plate is constant and can be obtained easily from the momentum equation which, for these particular conditions, reduces to

$$\frac{\tau_0}{\rho U_1^2} = \left(\frac{u_\tau}{U_1}\right)^2 = \frac{V_s}{U_1}.$$

As u_τ could be found, the asymptotic profiles have been plotted in the form u/u_τ vs. $\log_{10} u_\tau \rho y/\mu$, and the results compared with the accepted relationship for a solid flat plate. This comparison is made in Fig. 18. The two profiles are fairly close together in the laminar sub-layer region but as $u_\tau \rho y/\mu$ increases, they separate and form two roughly parallel straight lines, indicating that they obey a logarithmic law which is influenced by the nature of the surface. The gradient of the linear portion is quite different from that for the boundary layer without suction and is apparently independent of both the suction ratio and the geometry of the surface.

Another interesting feature is that the linear portion reaches almost to the outer edge of the boundary layer, just as in fully developed pipe flow it extends nearly to the centre of the pipe. In the turbulent boundary layer on a flat plate without suction this region extends only to about 0·28 from the surface. The different behaviour of the normal turbulent boundary layer and pipe flow, in this respect, have recently been attributed to the intermittent nature of the outer part of the boundary layer. Hence it is now suggested that in the turbulent asymptotic boundary layer this intermittency has been eliminated.

4.3. *The Mean-Flow Energy Balance.* It has been mentioned earlier (Section 4.1.2) that the Reynolds shear-stress distribution can be calculated through the asymptotic turbulent boundary layer. This suggested the possibility of using it in conjunction with the mean-flow energy equation to help to confirm some interesting results which have been obtained recently in turbulent boundary layers on a solid flat plate (*see* Refs. 7 and 8). The energy distribution is of interest because it may throw light on the nature of the turbulent flow in the boundary layer.

In the Appendix it is shown that for the turbulent asymptotic boundary layer the energy equation can be reduced to

$$\tfrac{1}{2}\sqrt{\frac{U_1}{V_s}} = \int_0^\infty \left(\frac{\mu}{\rho}\right)^2 \left(\frac{du}{dy}\right)^2 \frac{1}{u_\tau^4}\, dy^* - \int_0^\infty \left(\frac{\mu}{\rho}\right) \frac{1}{u_\tau^4} \overline{u'v'} \left(\frac{du}{dy}\right) dy^*,$$

where

$$y^* = \frac{u_\tau \rho y}{\mu}.$$

The terms under the integral signs on the right-hand side of this equation can be interpreted physically in the following way:

$\left(\frac{\mu}{\rho}\right)^2 \frac{1}{u_\tau^4}\left(\frac{du}{dy}\right)^2$ is proportional to the rate per unit mass at which energy from the mean flow is directly dissipated by viscosity,

$\frac{\mu}{\rho}\frac{1}{u_\tau^4}\overline{u'v'}\left(\frac{du}{dy}\right)$ is proportional to the rate per unit mass at which mean flow energy goes into the production of turbulence.

The energy equation in the form given above therefore shows how the increase in energy in the boundary layer due to the suction is exactly balanced by the decrease due to viscous dissipation and the conversion of the mean flow energy into turbulent energy.

For this special form of turbulent boundary layer the skin friction is easily obtained from the momentum equation and hence, as the Reynolds shear-stress distribution can be calculated, both the viscous dissipation term and the turbulence production term can be expressed in terms of the measured quantities and du/dy as shown in Appendix.

The distribution of these terms can therefore be plotted through the boundary layer and Fig. 19 shows their variation in the region immediately adjacent to the wall. It shows that the very high viscous stresses close to the surface account for a considerable proportion of the total dissipation of energy, and in fact for these results, 75 per cent of the total energy lost by the mean flow is dissipated in this way. Only 25 per cent of the energy is converted into turbulent energy. Fig. 19 also emphasises the great importance of the very narrow region close to the wall; the dissipation due to viscosity and the production of turbulence are both reduced to a negligible amount at a value of $u_\tau \rho y/\mu = 70$, which represents less than one tenth of the boundary-layer thickness. This region, being so close to the surface, is perhaps the most difficult to explore experimentally but it is obviously of great fundamental importance.

For comparison, Fig. 19 also includes some results obtained by Klebanoff in a constant-pressure turbulent boundary layer without suction. The distribution of the above terms is in general similar, but the proportion of mean flow energy which is converted into turbulent energy is smaller for the asymptotic turbulent layer. Presumably this term will be reduced still further with increasing suction ratios until it disappears altogether and the laminar asymptotic boundary layer is reached. It might also be suggested that for any suction ratios greater than the critical one this turbulence production term will decay as the boundary layer progresses along the plate until it disappears and the laminar asymptotic layer is attained.

Finally, as all the terms in the energy equation can be evaluated, the right-hand side can be integrated numerically and the energy balance calculated. This was done, and the good agreement obtained provided a useful check on the accuracy of the measurements.

5. *General Conclusions.* The development of a turbulent boundary layer with uniformly distributed suction depends largely on the type of surface through which suction is applied and the state of the boundary layer at the commencement of suction. No evidence was found in the present investigation to show that a general asymptotic solution exists for this type of boundary layer, as there is for the corresponding laminar boundary-layer problem. However, for a particular set of entry conditions an asymptotic form of the turbulent boundary layer has been shown to exist for a certain critical suction velocity ratio, this suction ratio depending upon the nature of the porous surface. For suction ratios less than this critical value the boundary layer was found to grow

continuously and showed no evidence of approaching an asymptotic state, while for suction ratios greater than the critical the thickness continually decreased.

It has also been shown that by means of distributed suction on either a perforated or porous surface the boundary-layer thickness can be reduced to such an extent that the laminar asymptotic boundary layer can be obtained from an initially turbulent layer. This laminar state is approached relatively slowly and requires a high suction ratio ($V_s/U_1 \doteq 0{\cdot}01$). However, it is apparent that comparatively small amounts of suction, *i.e.*, suction ratios in the region of $0{\cdot}004$, considerably reduce the turbulent boundary-layer thickness on both types of surface, the reduction being somewhat greater (at a particular R_x) on the smooth than on the perforated surface. The large change produced in the profile shape by small amounts of suction is qualitatively in accordance with the results of the numerous tests made elsewhere, showing that suction can usefully be employed to delay or prevent separation when the pressure gradient is adverse. Ultimately it may be hoped that some theory will be found to correlate quantitatively the zero pressure-gradient results with those obtained in adverse pressure gradients, but before such a theory can be developed it is obvious that many more experimental data are required, not only in adverse pressure gradients but also with zero pressure gradient. The dependence of the boundary-layer development on the nature of the surface and on entry conditions indicates that the behaviour of the boundary layer will also vary with Reynolds number and hence it is important that this should be systematically studied. For perforated surfaces the effects of hole spacing as well as hole diameter will have to be considered.

For truly asymptotic conditions the boundary-layer equations and the momentum and energy equations are greatly simplified, and the following conclusions are derived from the asymptotic velocity profiles obtained on the two surfaces considered.

The asymptotic profile is found to obey a logarithmic law, although this is very different from the logarithmic inner law for the ordinary turbulent boundary layer without suction. If the law is represented by

$$\frac{u}{u_\tau} = A \log_{10} \frac{u_\tau \rho y}{\mu} + B,$$

then B is affected by the nature of the surface, as for the turbulent boundary layer without suction, but the gradient A, although quite different from the corresponding gradient for zero suction, appears to be independent of both suction ratio and the type of surface. It is also interesting to note that the logarithmic law is applicable to the complete asymptotic profile and not just the inner fifth as it is without suction. This is a characteristic of fully developed turbulent pipe flow. Recently it has been suggested that this difference between the pipe and boundary-layer profiles is due to the intermittent nature of the outer part of the boundary layer, and it is now suggested that for some reason this intermittency has been eliminated in the asymptotic turbulent boundary layer.

The distribution of Reynolds stress through the asymptotic layer can be calculated, and this is found to be quite different from the distribution in the ordinary unsucked boundary layer. With the calculation of the Reynolds stress distribution the terms appearing in the boundary-layer energy equation can be evaluated. The rate of loss of mean flow energy has been plotted through the boundary layer and a result obtained from hot-wire measurements in boundary layers without suction, namely, that the very thin region adjacent to the boundary is a region of high dissipation, is confirmed.

The rate of turbulence production is found to be appreciably less for the asymptotic layer than it is for the unsucked boundary layer and it is suggested that with increasing suction ratios it will continue to decrease until it eventually vanishes and the laminar asymptotic boundary layer is reached.

NOTATION

ρ Density of air

μ Viscosity of air

τ_0 Shearing stress at the wall

P_0 Static pressure at reference position in working-section

p Local static pressure on flat plate

V_s Mean suction velocity through the surface

U_1 Mean velocity in free stream just outside boundary layer

$q_1 = \frac{1}{2}\rho U_1^2$ (Dynamic pressure in free stream just outside boundary layer)

q_0 Dynamic pressure in free stream at a reference station in tunnel working-section

u Mean velocity at any height in boundary layer

$u_\tau = \sqrt{\frac{\tau_0}{\rho}}$

u' Instantaneous fluctuating velocity component in streamwise direction

v' Instantaneous fluctuating velocity component in direction normal to free stream

$\overline{\rho u'v'}$ Reynolds shear stress

x Distance along plate from leading edge

y Vertical distance above surface

d Diameter of hole in surface

δ Boundary-layer thickness

$\delta^* = \int_0^\infty \left(1 - \frac{u}{U_1}\right) dy$ (Boundary-layer displacement thickness)

$\theta = \int_0^\infty \frac{u}{U_1}\left(1 - \frac{u}{U_1}\right) dy$ (Boundary-layer momentum thickness)

θ_0 Boundary-layer momentum thickness at commencement of suction

$\epsilon = \int_0^\infty \frac{u}{U_1}\left[1 - \left(\frac{u}{U_1}\right)^2\right] dy$ (Boundary-layer energy thickness)

$H = \frac{\delta^*}{\theta}$ Form parameter

$R_x = \frac{U_1 \rho x}{\mu}$

$R_\theta = \frac{U_1 \rho \theta}{\mu}$

$R_{\theta\,\infty}$ Asymptotic value of R_θ

$y^* = \frac{u_\tau \rho y}{\mu}$

P Non-dimensional parameter describing hole pattern in surface of flat plate

REFERENCES

No.	*Author*	*Title, etc.*
1	G. V. Lachman	Boundary-layer control. *J. R. Aer. Soc.* Vol. 59. pp. 163 to 198. March, 1955.
2	H. Schlichting	The boundary layer of the flat plate under conditions of suction and air injection. (*L.F.F.* Vol. 19, No. 9. October, 1942, pp. 293 to 301.) A.R.C. 6634. April, 1943.
3	J. M. Kay	Boundary-layer flow along a flat plate with uniform suction. R. & M. 2628. May, 1948.
4	A. A. Griffith and F. N. Meredith	The possible improvement in aircraft performance due to the use of boundary-layer suction. A.R.C. 2315. March, 1936.
5	R. A. Dutton	The asymptotic turbulent boundary layer. Readers Forum, *J. Ae. Sci.* Vol. 23. pp. 1127 to 1128. December, 1956.
6	M. R. Head	The boundary layer with distributed suction. R. & M. 2783. April, 1951.
7	P. S. Klebanoff	Characteristics of turbulence in a boundary layer with zero pressure gradient. N.A.C.A. Tech. Note 3178. July, 1954.
8	A. A. Townsend	The structure of the turbulent boundary layer. *Proc. Camb. Phil. Soc.* Vol. 47. Part 2. April, 1951.

APPENDIX

The Energy Equation and the Mean-Flow Energy Balance Calculated for the Turbulent Asymptotic Boundary Layer

The equation of motion for a turbulent boundary layer can be written

$$\frac{u\partial u}{\partial x} + V\frac{\partial u}{\partial y} = U_1\frac{dU_1}{dx} + \frac{1}{\rho}\frac{\partial \tau}{\partial y}, \tag{1}$$

where $\tau = \mu\frac{\partial u}{\partial y} - \overline{\rho u'v'}$, the total shear stress. The continuity equation is

$$\frac{\partial u}{\partial x} + \frac{\partial v}{\partial y} = 0. \tag{2}$$

Adding $\frac{u}{2}\left(\frac{\partial u}{\partial x} + \frac{\partial v}{\partial y}\right)$ to the left-hand side of equation (1), multiplying throughout by u and integrating from $y = 0$ to $y = \infty$ gives:

$$\int_0^\infty \frac{3}{2}u^2\frac{\partial u}{\partial x}\,dy + \int_0^\infty uv\frac{\partial u}{\partial y}\,dy + \int_0^\infty \frac{1}{2}u^2\frac{\partial v}{\partial y}\,dy - U_1\int_0^\infty u\frac{dU_1}{dx}\,dy = \frac{1}{\rho}\int_0^\infty u\frac{\partial \tau}{\partial y}\,dy.$$

Now

$$\frac{d}{dx}\int_0^\infty \frac{1}{2}(u^3 - uU_1^2)\,dy = \int_0^\infty \frac{3}{2}u^2\frac{\partial u}{\partial y}\,dy - U_1\int_0^\infty u\frac{dU_1}{dx}\,dy - \frac{U_1^2}{2}\int_0^\infty \frac{\partial u}{\partial x}\,dy.$$

Therefore

$$\frac{d}{dx}\int_0^\infty \frac{1}{2}(u^3 - uU_1^2)\,dy + \frac{U_1^2}{2}\int_0^\infty \frac{\partial u}{\partial y}\,dy + \left[\frac{u^2v}{2}\right]_0^\infty - \int_0^\infty \frac{u^2}{2}\frac{\partial v}{\partial y}\,dy + \int_0^\infty \frac{u^2}{2}\frac{\partial v}{\partial y}\,dy = \frac{1}{\rho}\int_0^\infty u\frac{\partial \tau}{\partial y}\,dy.$$

Also

$$v = \int_0^\infty \frac{\partial v}{\partial y}\,dy - V_s,$$

where V_s = suction velocity.

Therefore

$$\frac{d}{dx}\left[\frac{U_1^3}{2}\int_0^\infty \frac{u}{U_1}\left(1 - \frac{u^2}{U_1^2}\right)dy\right] - \frac{U_1^2}{2}\int_0^\infty \frac{\partial u}{\partial x}\,dy - \frac{1}{2}U_1^2\left[\int_0^\infty \frac{\partial v}{\partial y}\,dy - V_s\right] = \frac{1}{\rho}\times[u\tau]_0^\infty + \frac{1}{\rho}\int_0^\infty \tau\frac{\partial u}{\partial y}\,dy.$$

If $\int_0^\infty \frac{u}{U_1}\left(1 - \frac{u^2}{U_1^2}\right)dy$ is taken to define an energy thickness ϵ of the boundary layer, then:

$$\frac{1}{2}\frac{d}{dx}(\epsilon U_1^3) + \frac{1}{2}V_sU_1^2 = \frac{1}{\rho}\int_0^\infty \tau\frac{\partial u}{\partial y}\,dy = -\frac{1}{\rho}\int_0^\infty u\frac{\partial \tau}{\partial y}\,dy.$$

Therefore

$$\frac{1}{2}U_1^3\frac{d\epsilon}{dx} + \frac{3}{2}\epsilon U_1^2\frac{dU_1}{dx} + \frac{1}{2}V_sU_1^2 = \frac{1}{\rho}\int_0^\infty \tau\frac{\partial u}{\partial y}\,dy. \tag{3}$$

This is the energy equation for a turbulent boundary layer. For the asymptotic turbulent boundary layer, in which the pressure gradient is zero and the profile shape is independent of x, the equation (3) reduces to

$$\frac{1}{2}\frac{V_s}{U_1} = \frac{1}{\rho U_1^3}\int_0^\infty \tau \frac{\partial u}{\partial y}\,dy\,. \tag{3a}$$

Substituting now the full expression for τ,

$$\frac{1}{2}\frac{V_s}{U_1} = \frac{1}{\rho U_1^3}\int_0^\infty \mu\left(\frac{\partial u}{\partial y}\right)^2 dy - \frac{1}{\rho U_1^3}\int_0^\infty \rho\overline{u'v'}\frac{\partial u}{\partial y}\,dy$$

$$= \frac{1}{\rho U_1^3}\int_0^\infty \frac{\mu^2}{\rho u_\tau}\left(\frac{\partial u}{\partial y}\right)^2 dy^* - \frac{1}{U_1^3}\int_0^\infty \frac{\overline{u'v'}}{u_\tau}\frac{\mu}{\rho}\left(\frac{\partial u}{\partial y}\right) dy^*\,.$$

Therefore

$$\frac{1}{2}\frac{V_s}{U_1}\times\left(\frac{U_1}{u_\tau}\right)^3 = \int_0^\infty \frac{\mu^2}{\rho^2}\frac{1}{u_\tau^4}\left(\frac{\partial u}{\partial y}\right)^2 dy^* - \int_0^\infty \frac{\mu}{\rho}\frac{\overline{u'v'}}{u_\tau^4}\left(\frac{\partial u}{\partial y}\right) dy^*\,,$$

where $y^* = u_\tau \rho y/\mu$.

The two terms on the right-hand side represent the direct dissipation term (due to viscosity) and the turbulence-production term.

To calculate the magnitude of these terms for any value of y^* it is necessary to know (*a*) the skin friction and hence u_τ and (*b*) the value of $\overline{u'v'}$.

(*a*) The skin friction is obtained easily from the momentum equation, which for this particular set of conditions reduces to

$$\frac{\tau_0}{\rho U_1^2} = \left(\frac{u_\tau}{U_1}\right)^2 = \frac{V_s}{U_1}. \tag{4}$$

Thus

$$y^* = \frac{U_1 \rho y}{\mu}\sqrt{\frac{V_s}{U_1}}.$$

(*b*) To calculate the distribution of the Reynolds stress it is necessary to consider again the equation of motion for a turbulent boundary layer,

$$u\frac{\partial u}{\partial x} + v\frac{\partial u}{\partial y} = U_1\frac{dU_1}{dx} + \frac{1}{\rho}\frac{\partial \tau}{\partial y}\,. \tag{1}$$

For the asymptotic condition in zero pressure gradient this reduces to

$$-V_s\frac{\partial u}{\partial y} = \frac{1}{\rho}\frac{\partial \tau}{\partial y}\,.$$

Therefore

$$-V_s[u]_0^y = \frac{1}{\rho}[\tau]_0^y\,.$$

Therefore

$$-\rho V_s u = \tau - \tau_0\,.$$

Now from the modified momentum equation (4)

$$\tau_0 = \rho V_s U_1\,.$$

Therefore

$$\tau = \rho V_s U_1\left(1 - \frac{u}{U_1}\right), \tag{5}$$

which gives the distribution of total shear stress through the boundary layer.

Hence

$$-\overline{u'v'} = V_s U_1 \left(1 - \frac{u}{U_1}\right) - \frac{\mu}{\rho}\frac{\partial u}{\partial y}$$

or

$$\frac{\overline{u'v'}}{u_\tau^2} = \frac{1}{u_\tau^2}\frac{\mu}{\rho}\frac{\partial u}{\partial y} - \left(1 - \frac{u}{U_1}\right). \tag{6}$$

The velocity gradient through the boundary layer can be computed from the velocity profile and hence the distribution of Reynolds shear stress can be found.

The direct dissipation term and the production term can now be calculated from the measured results in the following way:

The direct dissipation term is

$$\left(\frac{\mu}{\rho}\right)^2 \frac{1}{u_\tau^4}\left(\frac{du}{dy}\right)^2 \equiv \left(\frac{\mu}{U_1\rho}\right)^2 \times \left(\frac{U_1}{V_s}\right)^2 \times \left(d\frac{u}{U_1}{dy}\right)^2.$$

Similarly, using equation (6), the turbulence production term can be expressed as

$$\frac{\mu}{\rho}\frac{\overline{u'v'}}{u_\tau^4}\frac{du}{dy} \equiv \frac{\mu}{\rho U_1} \times \frac{U_1^2}{u_\tau^2} \times \frac{d\frac{u}{U_1}}{dy}\left[\frac{U_1^2}{u_\tau^2}\frac{\mu}{U_1\rho}\frac{d\frac{u}{U_1}}{dy} - \left(1 - \frac{u}{U_1}\right)\right]$$

$$= \left[D.D. - \sqrt{D.D.}\left(1 - \frac{u}{U_1}\right)\right],$$

where $D.D.$ = direct dissipation term.

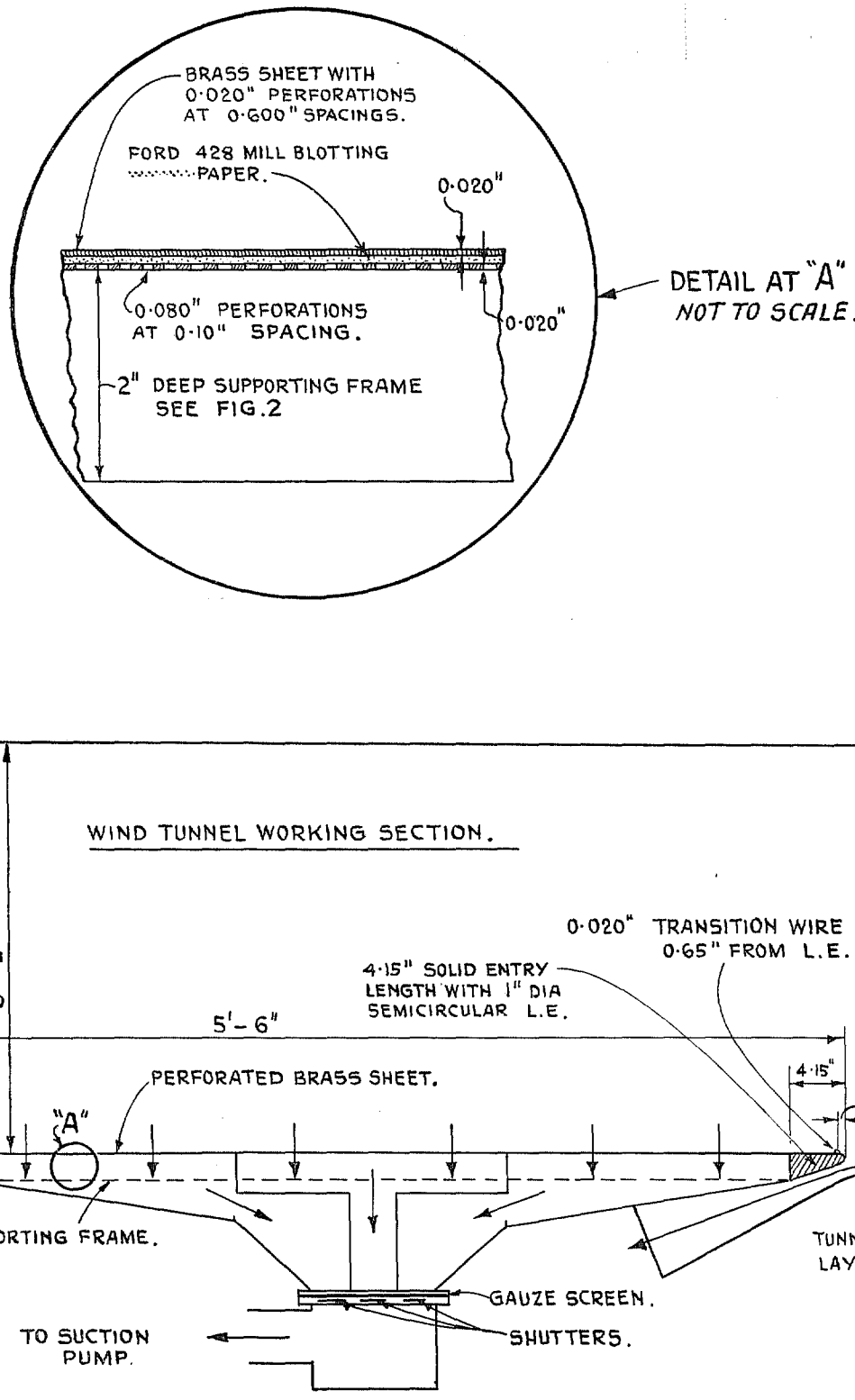

FIG. 1. General arrangement of suction apparatus.

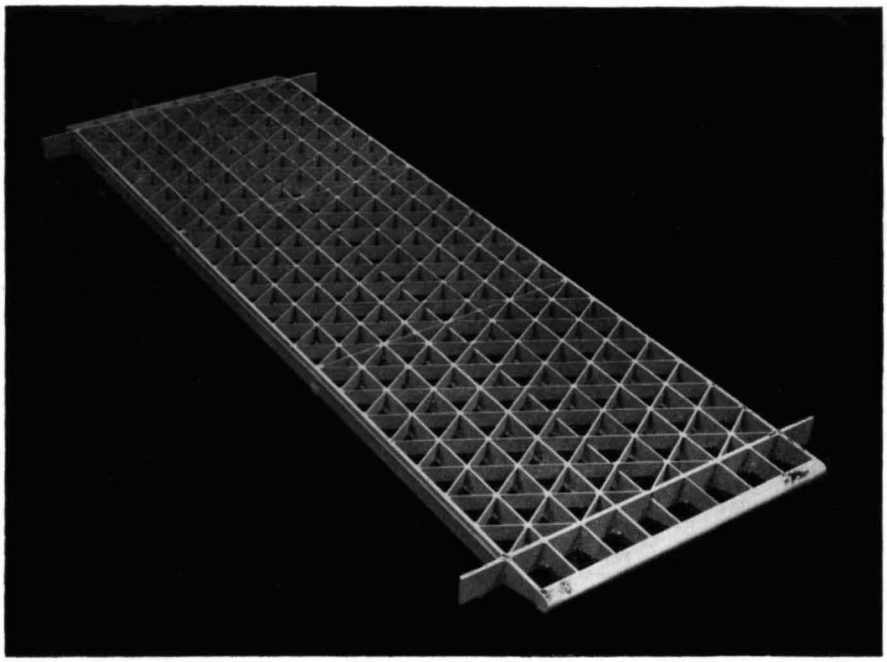

FIG. 2. Supporting framework used in construction of a porous surface through which suction was applied.

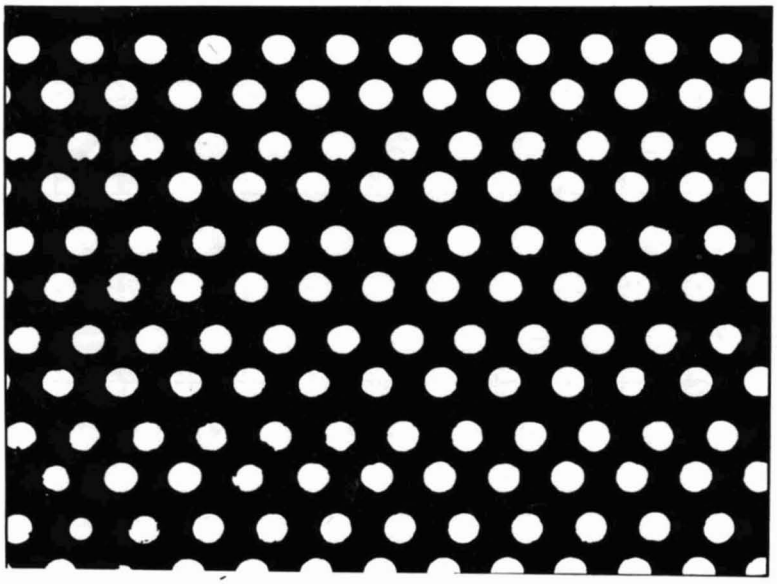

FIG. 3. Photograph of perforated brass sheet—Magnification 10 times.

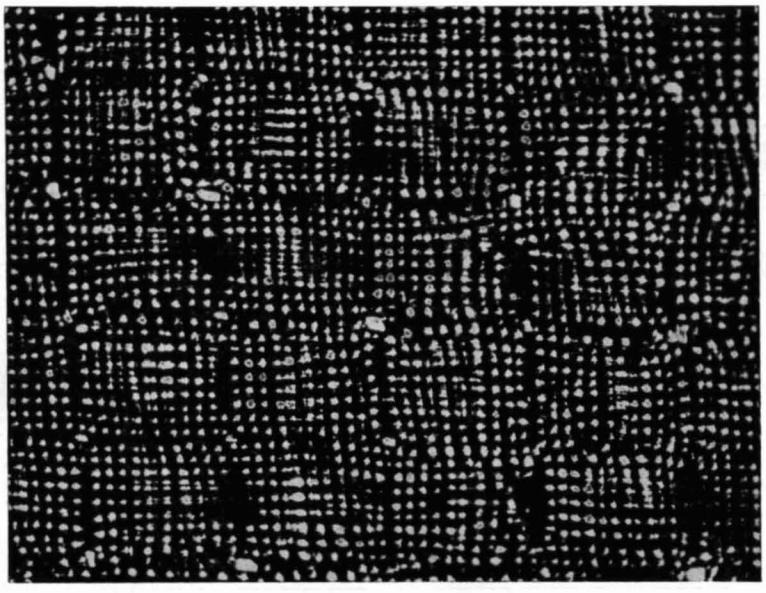

FIG. 4. Photograph of calendered nylon—Magnification 75 times.

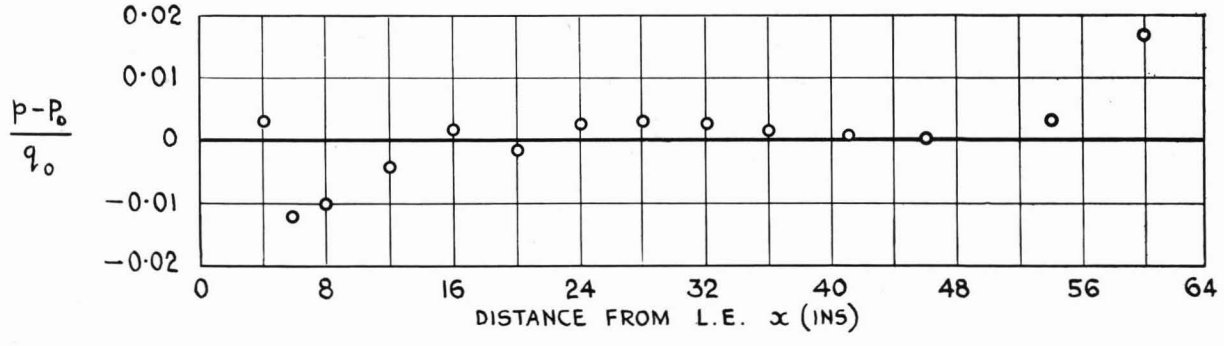

FIG. 5. Pressure distribution along perforated flat plate.

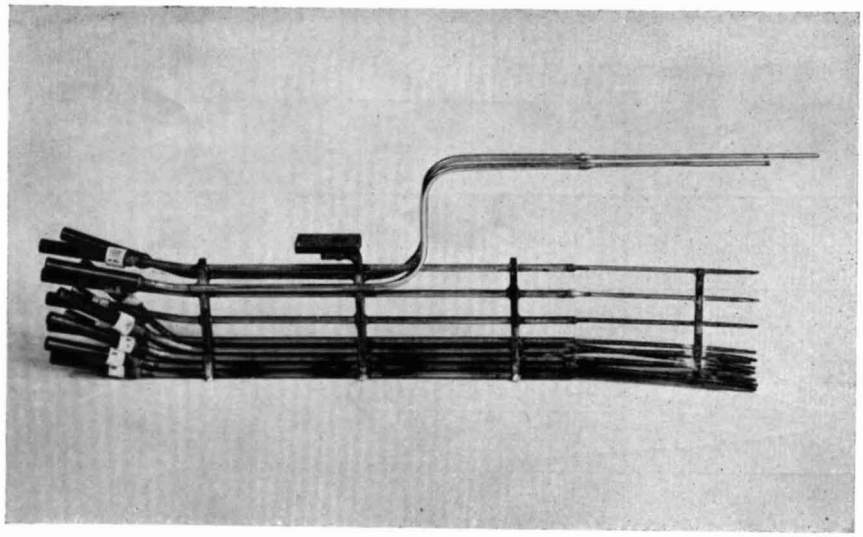

FIG. 6. Pitot comb.

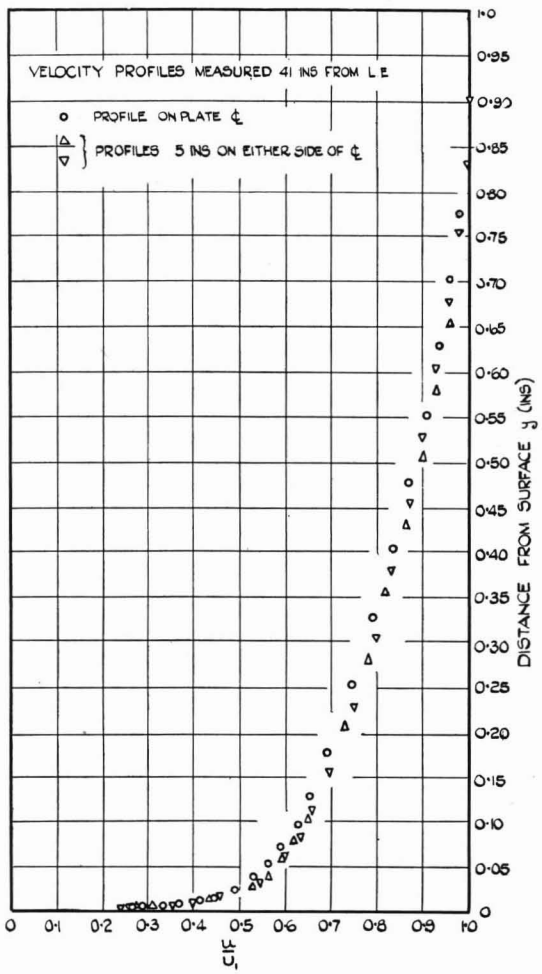

FIG. 7. Velocity profiles measured at spanwise positions on the flat perforated plate with zero suction.

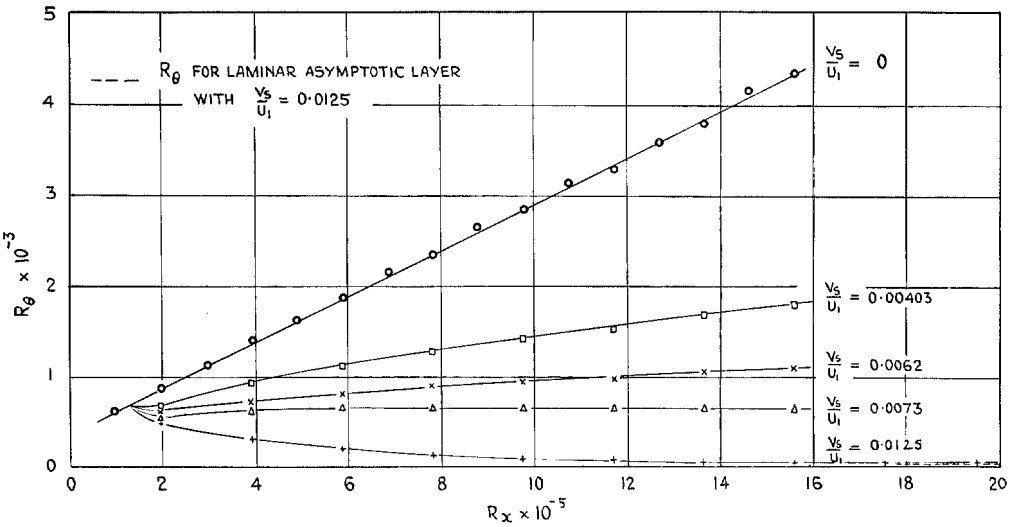

FIG. 8. The development of an initially turbulent boundary layer for various rates of suction through a perforated surface.

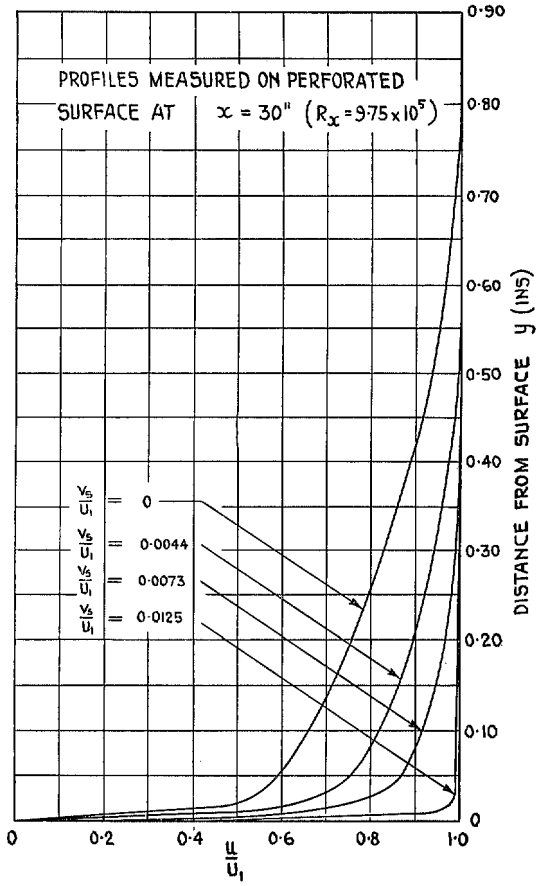

FIG. 9. The change in velocity profile shape with increasing values of V_s/U_1.

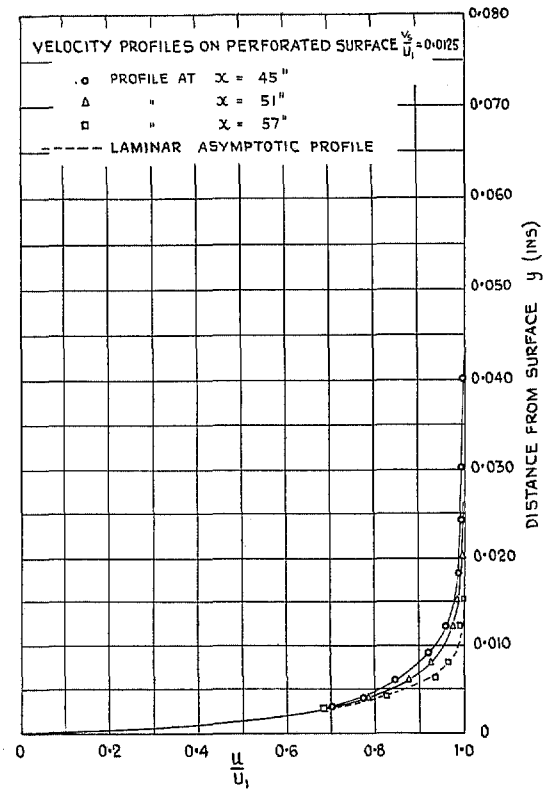

FIG. 10. A laminar asymptotic velocity profile from an initially turbulent boundary layer.

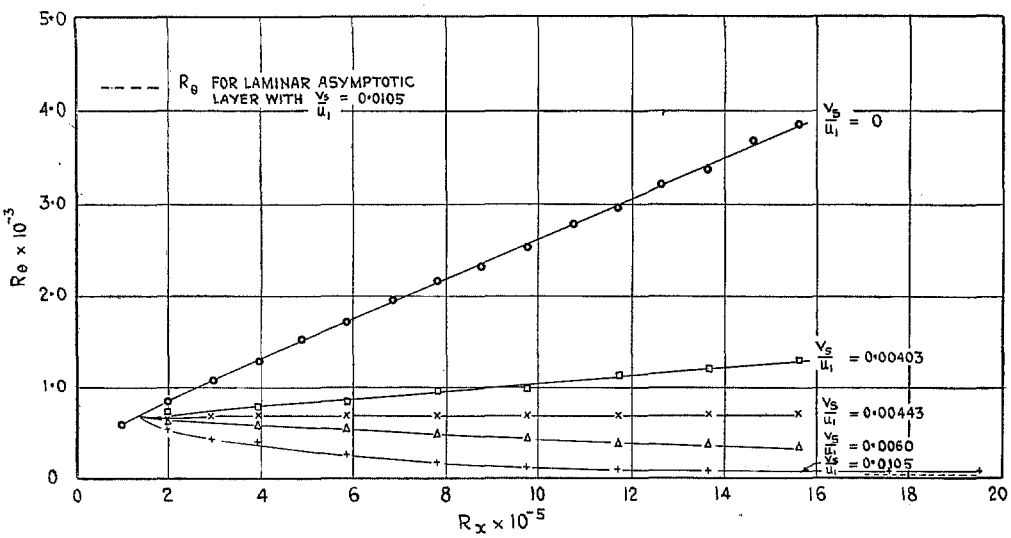

FIG. 11. The development of an initially turbulent boundary layer for various rates of suction through the nylon-covered surface.

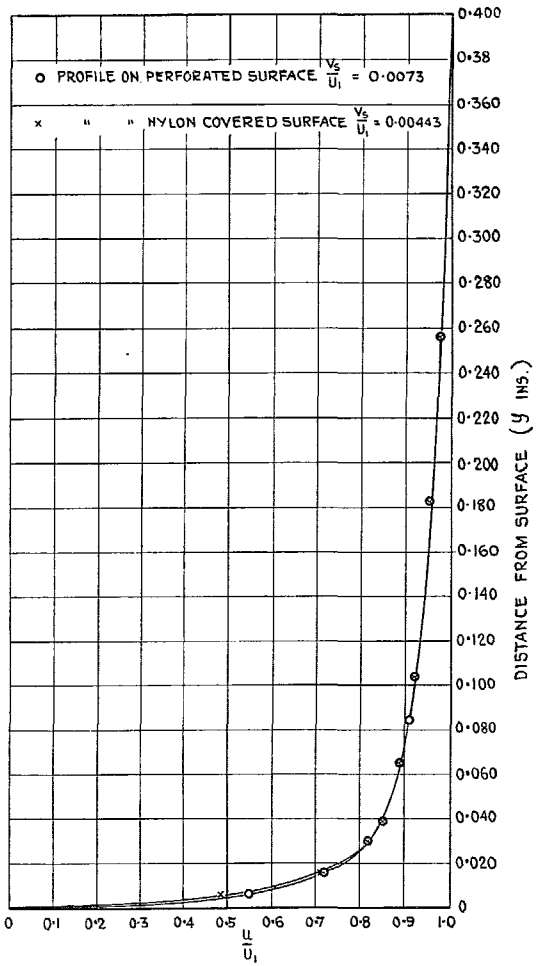

FIG. 12. Asymptotic turbulent velocity profiles on the perforated and nylon-covered surfaces.

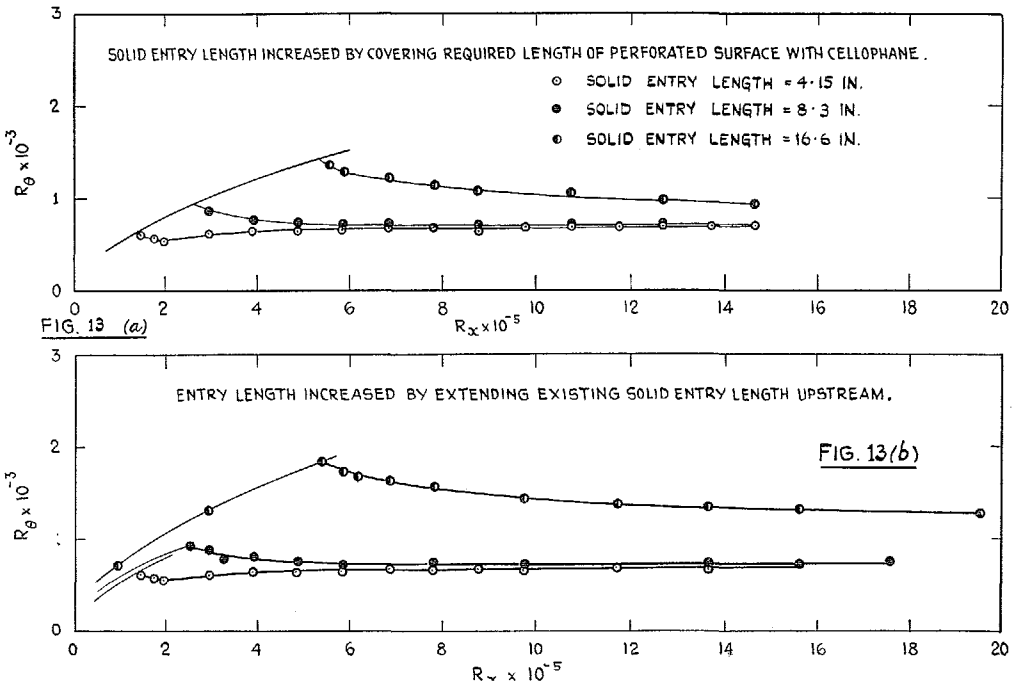

FIGS. 13a and 13b. The influence of entry conditions and the critical suction ratio on the development of the turbulent boundary layer along the perforated surface ($V_s/U_1 = 0{\cdot}0073$).

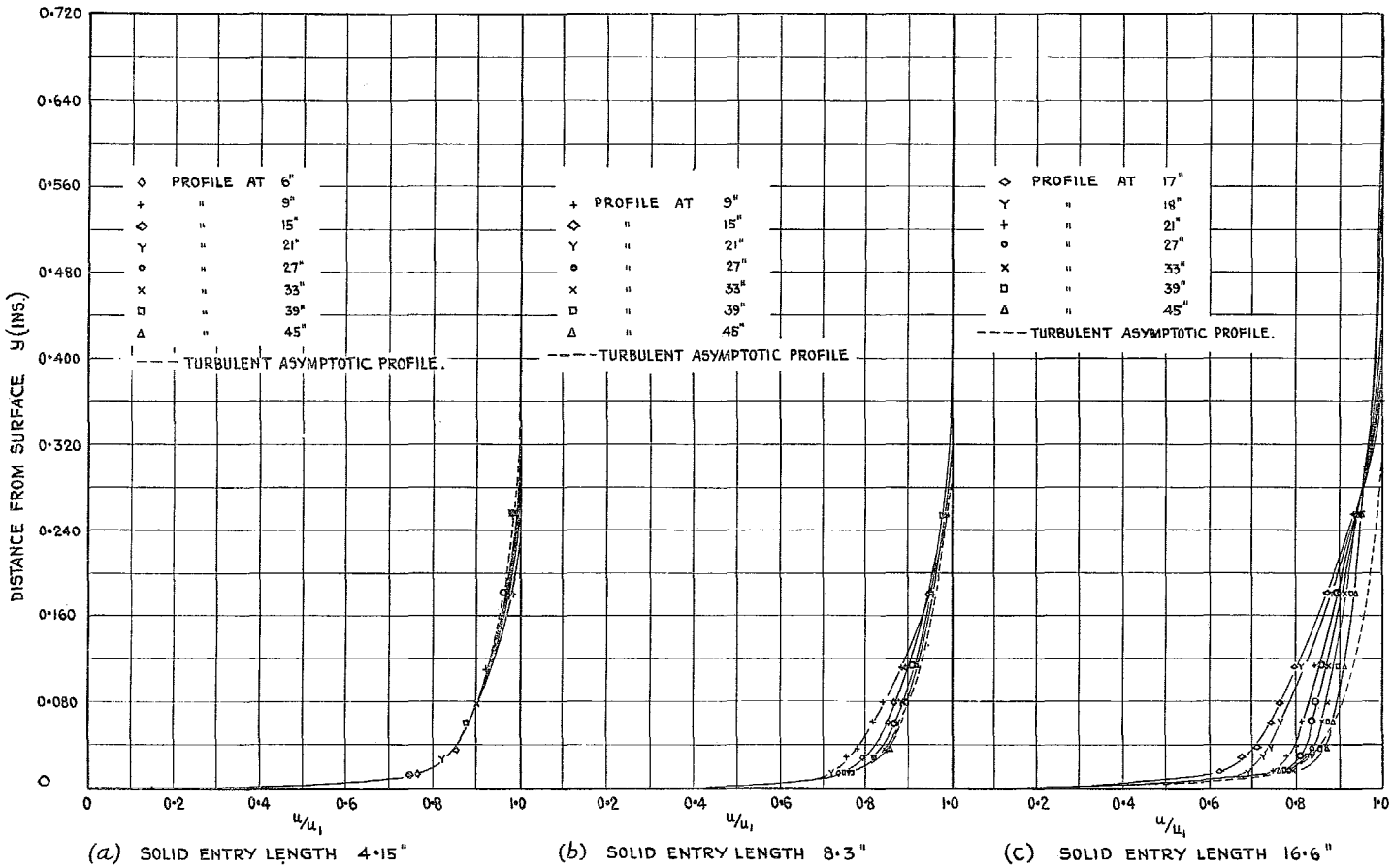

FIGS. 14a to 14c. Velocity profiles on perforated surface with the critical suction ratio ($V_s/U_1 = 0{\cdot}0073$) and different solid entry lengths.

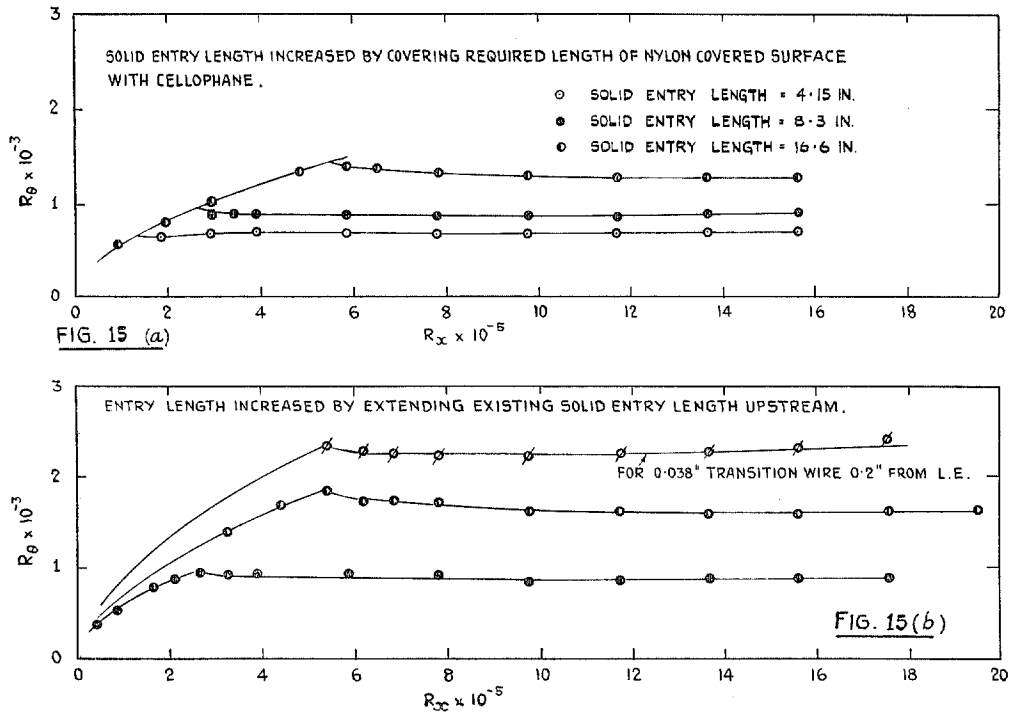

FIGS. 15a and 15b. The influence of entry conditions and the critical suction ratio on the development of the turbulent boundary layer along the nylon-covered surface.

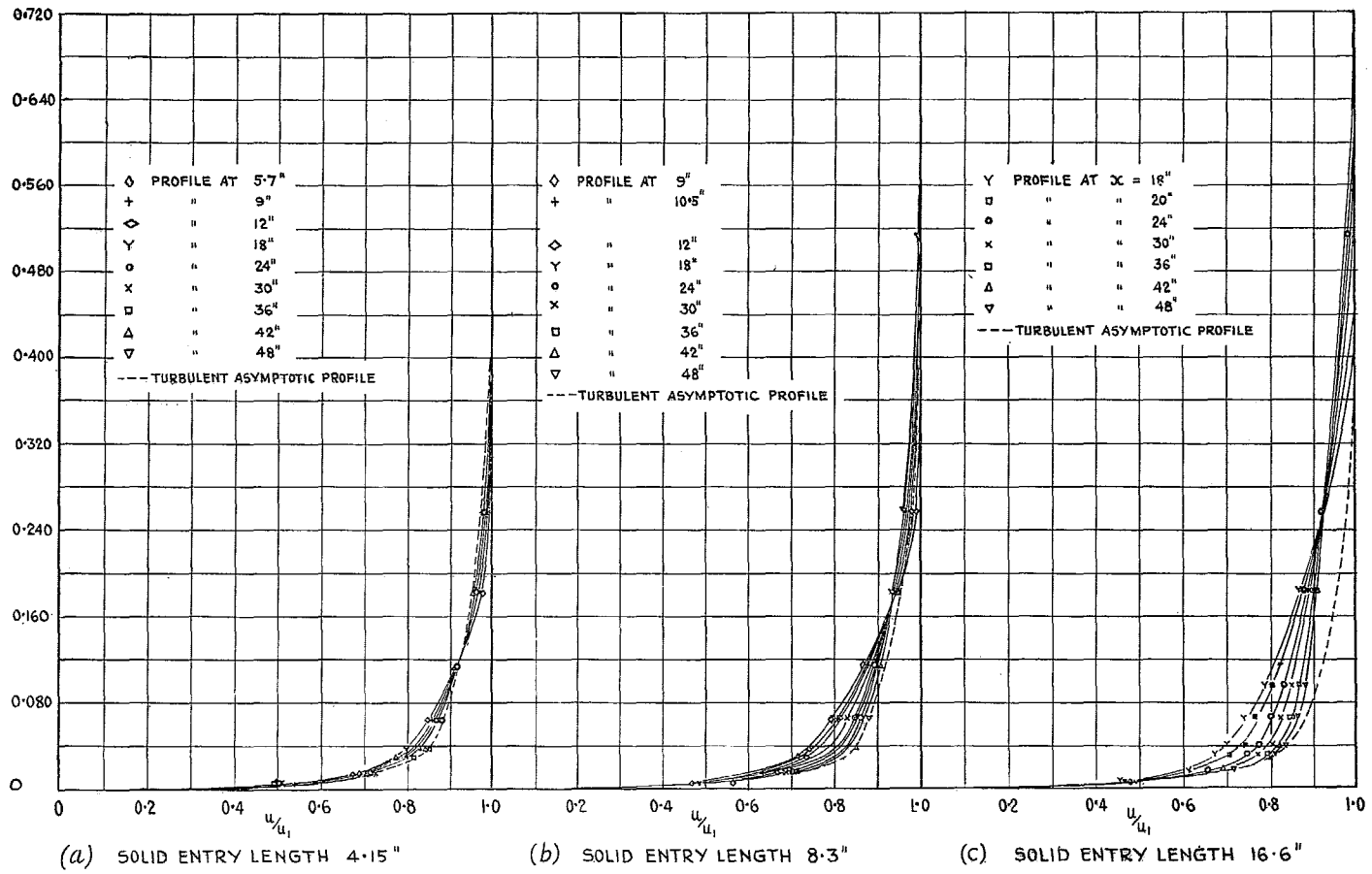

FIGS. 16a to 16c. Velocity profiles on nylon-covered surface with the critical suction ratio ($V_s/U_1 = 0{\cdot}00443$) and different solid entry lengths.

(78644) Wt. 54/8210 K.5 10/60 Hw.

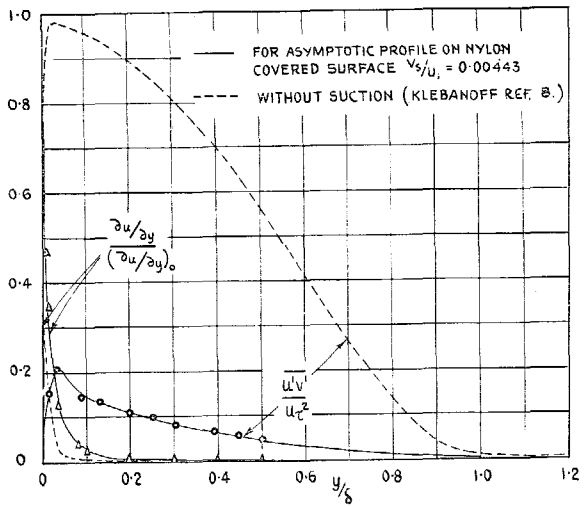

FIG. 17. Comparison between viscous and Reynolds stress distribution in a turbulent boundary layer with and without suction.

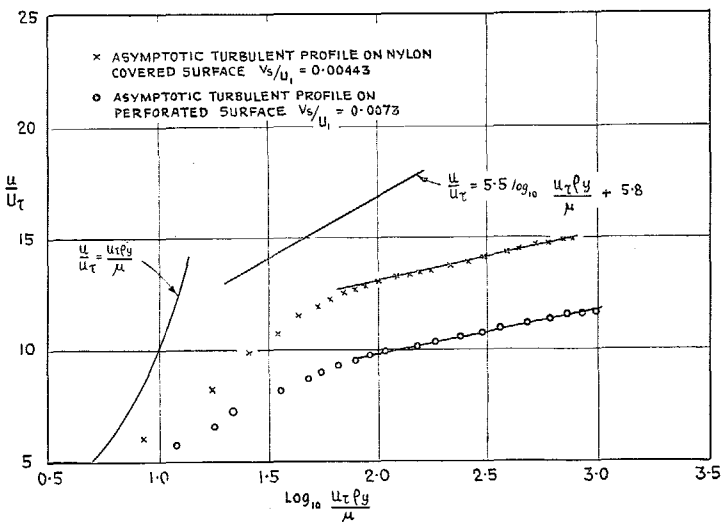

FIG. 18. Comparison between the logarithmic plotting of the complete asymptotic profiles and the 'inner' law for flat plates.

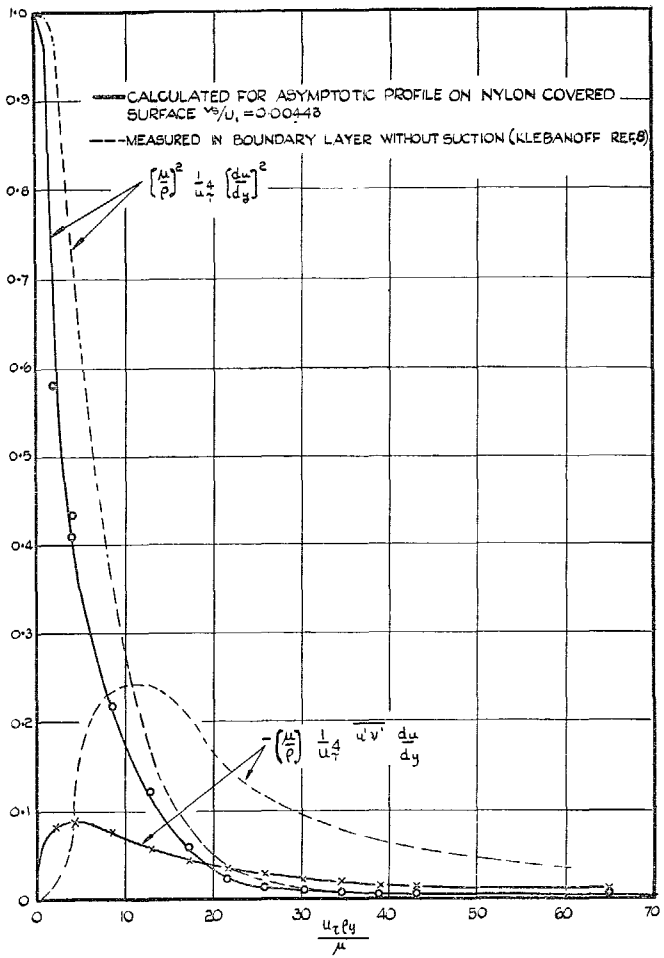

FIG. 19. Rate of loss of mean flow energy in turbulent boundary layer with and without distributed suction.

Publications of the Aeronautical Research Council

ANNUAL TECHNICAL REPORTS OF THE AERONAUTICAL RESEARCH COUNCIL (BOUND VOLUMES)

1941 Aero and Hydrodynamics, Aerofoils, Airscrews, Engines, Flutter, Stability and Control, Structures. 63*s.* (post 2*s.* 3*d.*

1942 Vol. I. Aero and Hydrodynamics, Aerofoils, Airscrews, Engines. 75*s.* (post 2*s.* 3*d.*)

Vol. II. Noise, Parachutes, Stability and Control, Structures, Vibration, Wind Tunnels. 47*s.* 6*d.* (post 1*s.* 9*d.*)

1943 Vol. I. Aerodynamics, Aerofoils, Airscrews. 80*s.* (post 2*s.*)

Vol. II. Engines, Flutter, Materials, Parachutes, Performance, Stability and Control, Structures. 90*s.* (post 2*s.* 3*d.*)

1944 Vol. I. Aero and Hydrodynamics, Aerofoils. Aircraft. Airscrews, Controls. 84*s.* (post 2*s.* 6*d.*)

Vol. II. Flutter and Vibration, Materials, Miscellaneous, Navigation, Parachutes, Performance, Plates and Panels, Stability, Structures, Test Equipment, Wind Tunnels. 84*s.* (post 2*s.* 6*d.*)

1945 Vol. I. Aero and Hydrodynamics, Aerofoils. 130*s.* (post 2*s.* 9*d.*)

Vol. II. Aircraft, Airscrews, Controls. 130*s.* (post 2*s.* 9*d.*)

Vol. III. Flutter and Vibration, Instruments, Miscellaneous, Parachutes, Plates and Panels, Propulsion. 130*s.* (post 2*s.* 6*d.*)

Vol. IV. Stability, Structures, Wind Tunnels, Wind Tunnel Technique. 130*s.* (post 2*s.* 6*d.*)

Special Volumes

Vol. I. Aero and Hydrodynamics, Aerofoils, Controls, Flutter, Kites, Parachutes, Performance, Propulsion, Stability. 126*s.* (post 2*s.* 6*d.*)

Vol. II. Aero and Hydrodynamics, Aerofoils, Airscrews, Controls, Flutter, Materials, Miscellaneous, Parachutes, Propulsion, Stability, Structures. 147*s.* (post 2*s.* 6*d.*)

Vol. III. Aero and Hydrodynamics, Aerofoils, Airscrews, Controls, Flutter, Kites, Miscellaneous, Parachutes, Propulsion, Seaplanes, Stability, Structures, Test Equipment. 189*s.* (post 3*s.* 3*d.*)

Reviews of the Aeronautical Research Council

1939–48 3*s.* (post 5*d.*) 1949–54 5*s.* (post 6*d.*)

Index to all Reports and Memoranda published in the Annual Technical Reports

1909–1947 R. & M. 2600 6*s.* (post 4*d.*)

Author Index to the Reports and Memoranda and Current Papers of the Aeronautical Research Council

February, 1954–February, 1958 R & M. No. 2570 (Revised) (Addendum) 7*s.* 6*d.* (post 4*d.*)

Indexes to the Technical Reports of the Aeronautical Research Council

July 1, 1946–December 31, 1946 R. & M. No. 2150 1*s.* 3*d.* (post 2*d.*)

Published Reports and Memoranda of the Aeronautical Research Council

Between Nos. 2251–2349	R. & M. No. 2350 1*s.* 9*d.* (post 2d.)
Between Nos. 2351–2449	R. & M. No. 2450 2*s.* (post 2*d.*)
Between Nos. 2451–2549	R. & M. No. 2550 2*s.* 6*d.* (post 2*d.*)
Between Nos. 2551–2649	R. & M. No. 2650 2*s.* 6*d.* (post 2*d.*)
Between Nos. 2651–2749	R. & M. No. 2750 2*s.* 6*d.* (post 2*d.*)
Between Nos. 2751–2849	R. & M. No. 2850 2*s.* 6*d.* (post 2*d.*)
Between Nos. 2851–2949	R. & M. No. 2950 3*s.* (post 2*d.*)

HER MAJESTY'S STATIONERY OFFICE

from the addresses overleaf

Printed and published by
HER MAJESTY'S STATIONERY OFFICE

To be purchased from
York House, Kingsway, London W.C.2
423 Oxford Street, London W.1
13A Castle Street, Edinburgh 2
109 St. Mary Street, Cardiff
39 King Street, Manchester 2
50 Fairfax Street, Bristol 1
2 Edmund Street, Birmingham 3
80 Chichester Street, Belfast 1
or through any bookseller

Printed in England

S.O. Code No. 23-3155